https://doi.org/10.20965/ijat.2017.p0442

Paper:

Elbow Musculoskeletal Model for Industrial Exoskeleton with Modulated Impedance Based on Operator's Arm Stiffness

Daniele Borzelli†, Stefano Pastorelli, and Laura Gastaldi

Politecnico di Torino
Corso Duca degli Abruzzi 24, 10129 Torino, Italy
†Corresponding author, E-mail: daniele.borzelli@polito.it
[Received October 1, 2016; accepted April 10, 2017]

With the ageing of the workforce in the manufacturing industry, the possibility of introducing support aids such as exoskeletons to reduce the fatigue and effort of the operator has to be evaluated. An upper-limb exoskeleton with controlled impedance is expected to reduce the discomfort in the operations which require precision. Hence, arm joint stiffening is required. Real-time calculation of the exoskeleton impedance should be based on the operator's limb impedance, evaluated through electromyographic signals. A model of the operator's arm is necessary to identify the best control law for the exoskeleton. In this paper, preliminary considerations and a model of the elbow on which two muscles act as agonist-antagonist are presented. Numerical results are discussed, and an estimation of the performance is also proposed.

Keywords: arm stiffness, hill muscle model, elbow model, exoskeleton

1. Exoskeleton Definition

Humans possess natural control of movement, but the exerted forces are limited by muscle strength. By contrast, robotic manipulators can perform tasks requiring high forces, but control algorithms do not provide the flexibility and quality of performance naturally achievable by humans. Exoskeletons, by interfacing human and robotic skills, might represent an interesting solution [1].

The definition of an exoskeleton is still debated [2]. Beyond the differences, the main characteristics identified by all the studies are that an exoskeleton is a wearable device that involves a direct man-machine interaction. The interaction is both from the robot to the human and from the human to the robot. The first is a result of the intrinsic characteristics of the exoskeleton, and is cognitive (exoskeleton gives feedback to the operator) and biomechanical (exoskeleton applies controlled forces on exoskeleton) [3]. The second one can be performed in different ways that define the exoskeleton generation. Three generations are identified [2]: the user controls the exoskeleton (1) with his/her kinematics, (2) in a dynamic way, and (3) with his/her neuromuscular signals, recorded with electromyography (EMG).

First-generation exoskeletons are used to assist human locomotion and to apply a set of predefined joint angle trajectories. An example of a position-based control exoskeleton is the Hardiman [4], developed for military purposes, which enhances performance. In exoskeletons of the second generation, two control strategies are commonly applied [5]. The first involves an open-loop control such that a pre-specified force or torque value is applied based on the position (i.e., portion of the gait cycle for lower limb exoskeletons). The second strategy consists of a control proportional to the force/torque exchanged between the user and the exoskeleton. Examples are BLEEX [6] for load carrying and ALEX [7] and ARMin [8] for rehabilitation.

An exoskeleton of the third generation was first developed for the upper limb [2]. Driving the exoskeleton using an EMG signal leads to a movement that feels more natural to the user since it is not necessary to exert an action on the exoskeleton. As a matter of fact, EMG signals appear approximately 20–80 ms prior to the muscles contracting mechanically [9], thus allowing a signal evaluation before the motion. EMG-based exoskeletons were developed for the upper and lower limbs.

Exoskeletons can also be classified according to their field of use. The first exoskeleton prototypes were developed for military purposes [4]. Another common application is in the rehabilitation field. Here, exoskeleton can enhance the force exerted by weak patients such as older people or patients with diseases that do not allow them to exert enough strength, or can assist physiotherapists during rehabilitation sessions [10]. Exoskeletons were also proposed as supports for agricultural workers or for back support. Recently, exoskeletons for industrial purposes [11, 12] are under consideration. Beneficial effects in terms of ergonomics and reduced fatigue are expected, especially during uncomfortable postures [13].

During manufacturing, some operations may require joint stiffening owing to unstable characteristics or requested high precision. In these operations, an amplification of the force exerted may not be necessary. However, the development of an exoskeleton (whose purpose is to increase the joints' stiffness without increasing the exerted end-point force) may have beneficial effects while performing different operations.

In this paper, we discuss some concepts for the development of an industrial exoskeleton for the upper limbs. The impedance of the exoskeleton is controlled in real time by recording the activation of the operator's muscles. While a force transducer can directly measure the force exerted by the operator, stiffness cannot be measured without applying a displacement. Thus, it needs to be calculated based on a recorded EMG. A model of the operator's arm is necessary to identify the best control law for the exoskeleton. For this purpose, a model of the arm, based on Hill's muscle model, was implemented. Analysis results are presented and discussed.

2. Exoskeletons and Arm Impedance

During working activity, the operator interacts with the environment and a large number of tools. When interactions are unstable, limb impedance modulation is required. Limb impedance is achieved by co-activating muscles. Different authors analyze arm impedance (inertia, damping, and stiffness) during dynamic [14, 15] and isometric tasks [16–18]. End-point stiffness is defined as the relationship between externally applied displacements of the hand and the forces generated in response [19, 20]. End-point stiffness is non-isotropic [21, 22] and can be graphically represented as an ellipse [23]. Muscle patterns that modulate stiffness are studied both during dynamic [24, 25] and isometric tasks [26, 27].

Many exoskeletons are developed with different kinds of impedance control, which is a method that modulates the high mechanical impedance arising in traditional stiff and high-inertia robotic manipulators and in impact management systems [28]. Impedance control is implemented in some rehabilitation exoskeletons to drive patient's limb [29, 30] or to reduce hand tremors [3]. However, the impedance of all these cases is not calculated from the user's limb impedance.

In the literature, robotic devices controlled by EMG signals are developed for safer human-machine interfaces or during robot operations when external forces are not known a priori. The impedance control of robotic devices based on a used EMG signal is developed by different groups [31–33]. Real-time impedance controls based on EMG signals are also developed for the modulation of the stiffness of the upper limb [34] prosthesis. In the HAL exoskeleton [35], the lower limbs assume different impedances depending on the phase of the gait. However, no exoskeletons whose stiffness is controlled directly by biological signals recorded from the operator have been developed for industrial use.

3. Task Definition

As previously described, modulation of stiffness is useful in different kinds of operations. The operations for which stiffness modulation is required can be classified based on the characteristics of the task. Two groups were identified.

- Isometric operations: needs the application of a force, without a movement requirement.
- Dynamic operations: movement requirement without the need of high-force application.

This classification came not only from a dynamic description of the task but also looks to be intrinsic in the Central Nervous System (CNS). As a matter of fact, although during dynamic tasks, the stiffness ellipse aligns with the direction of the instability (as observed for a ball-catching task [36] and a pointing task [37]), during isometric tasks only small rotations were observed [17, 38]. Another classification of the operations in which arm stiffening is required depended on the reason why the operator stiffens his arm. Two reasons were identified:

- External instability: the subject has a sensorimotor feedback of a displacement that may cause instability. The reasons for this instability can result from various causes: the device itself (e.g., rotational elements of the device's engine), the interaction of the device with another object (e.g., vibration owing to a drilling action), the environment in which the device is used (e.g., a windy environment), the operator's working conditions (e.g., a moving platform), or the operator's physiological tremors (e.g., fatigue).
- Predicted instability: the operator knows, by his experience, that some instabilities may occur, so he stiffens his joints to prevent instability. This behavior may occur when the work material is non-homogeneous (e.g., ribs on wood). The environment or the tool the operator is using may exert undesired actions (e.g., a drill press may make the object to be drilled escape from the operator's hand). Some actions may lead to unstable configurations (e.g., the exertion of a force with a screwdriver non-orthogonal to the plane). The behavior may also occur for security reasons (e.g., managing dangerous substances or devices whose incorrect use may lead to injuries).

The required stiffening of the arm can be along different directions: it can have the same force or of the movement direction , or it can assume different angles with respect to them. The combination of the kind of kinematic task and the cause of stiffening leads to the identification of different tasks in which the exoskeleton should operate. An iconic machining, together with the identification of the angle between the direction of the instabilities and the direction of the force, was identified for each group (**Fig. 1**):

- Isometric task, external instability: the use of a drill when it makes contact with the plane. There is no movement, but a force is required. The instability felt by the worker is a result of the interaction of the drill with the plane and the rotation of the drill's motor. Stiffness modulation is required to reduce vibration. The limb needs to be stiffened along all directions orthogonal to the drilling. No stiffening is

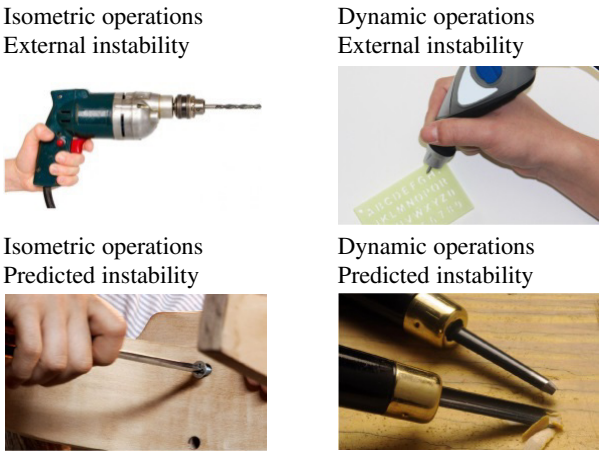

Fig. 1. Iconic machining of different tasks.

needed along the direction orthogonal to the plane (i.e., the direction of the application of the force).

- Dynamic task, external instability: engraving a plane with an electric tool. A movement is required, while no force is requested. The instability felt by the worker is a result of the rotation of the device's motor. Stiffness is required to reduce vibration. All directions orthogonal to the direction of the engraving are axes along which stiffening is required. No stiffening is needed along the direction of the engraving.

- Isometric task, predicted instability: the use of a screwdriver (when the screw is still outside the plane). There is no movement, but enough force is required to start the screwing. The instability derives from the coupling between the screw and the plane (e.g., if a force is exerted along a direction that is not precisely orthogonal to the plane, with the consequence of an instability). The operator stiffens the arm to prevent any instabilities that may occur. Stiffening is needed along directions orthogonal to the direction of the drilling, but no stiffness is required in directions parallel to the force.

- Dynamic task, predicted instability: engraving a plane by hand. A movement is required, but the force needs to be precisely modulated by the worker owing to the requested precision. The instability derives from the dis-homogeneities of the material of the plane to be engraved, and is predicted by the worker. The operator reduces the instabilities owing to dis-homogeneities by stiffening his limb along all directions orthogonal to the engraving direction. No stiffening is needed along the direction of the engraving.

As can be observed in each operation, if a movement or a force is exerted along a specific direction, the instability that needs to be compensated by a stiffening of the arm is commonly along an orthogonal direction. A stiffness increase along the movement, or the force exertion direction, may be harmful because it opposes the motion or reduces the exerted force. Thus, the system needs to select the directions in which an increase in stiffness is required, and reduce its stiffness along the others. For this reason, the knowledge of the arm stiffness the operator intends to exert needs to be as precise as possible.

4. Exoskeleton Concept

A diagram block of a man-machine interaction in case of an upperlimb exoskeleton whose impedance is controlled in real time by the recording of the activation of the operator's muscles is reported in **Fig. 2**. The CNS of the human operator activates muscles to produce force and stiffness of the arm. The selection of the muscle pattern is computed by the CNS and is based on both feedback and feedforward controls. The knowledge of the biological control implemented in the human CNS is still debated.

The force and stiffness exerted by the operator is computed on the basis of his/her muscle activations and the configuration of the arm ("Data Process" block). Once the force and stiffness required by the operator are known, the activation of the exoskeleton motors needs to be calculated ("Control" block). This operation can be separated into a first calculation of the force and stiffness that the exoskeleton needs to exert to reduce the user's muscle activation ("Control law" block), and a second calculation of the motor activations. This is accomplished using a model of the exoskeleton ("Exoskeleton model" block). The force and the stiffness exerted by the exoskeleton are combined with those of the operator to assess the endpoint force and stiffness.

5. Arm to Define Exoskeleton Control Law

The main focus of this study is to develop an arm model to assess the control law for the exoskeleton ("Control law" block of **Fig. 2**).

5.1. Arm Musculo-Tendon System Models

The arm model consisted of two rigid segments that represented the humerus bone and radio-ulna bones. They were connected by a single-degree-of-freedom hinge that corresponded to the elbow. Two actuators simulated the muscles Brachioradialis (BRD, muscle 1) and Lateral head of the Triceps (TriLat, muscle 2) acting on the joint (**Fig. 3**). The connections between the links and the actuators were made by hinges. The elbow angle α was assumed to be zero when the forearm was completely extended, and it increased with the flexion of the elbow.

The actuators were single effect: they exerted only pulling actions, one opposed to the other, and worked as a redundant drive [39, 40]. The musculo-tendon system was analytically described based on the Hill model, which is commonplace in the computational literature and a valid method to analyze feasible mechanical behavior. The Hill model [41] is composed of different elements (**Fig. 4A**).

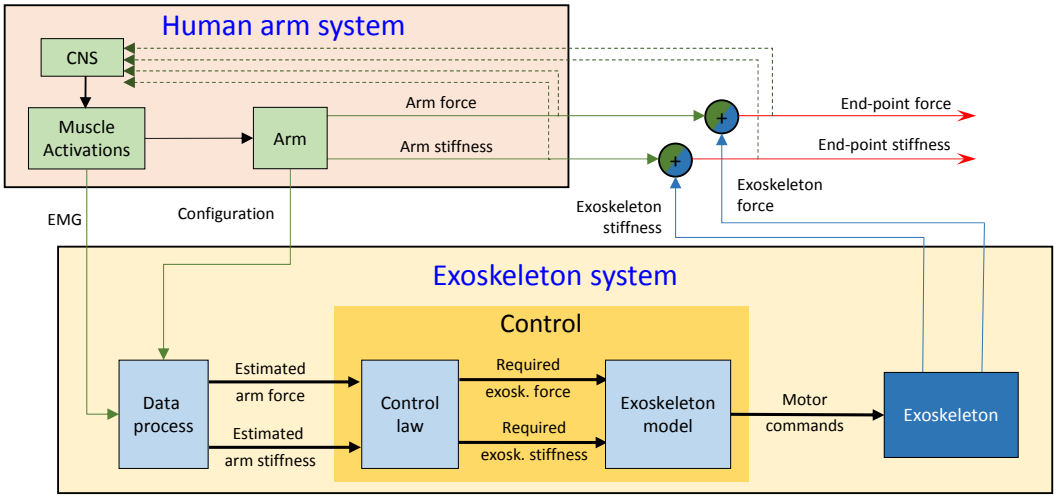

Fig. 2. Concept of exoskeleton that enhances end-point force and stiffness of the operator.

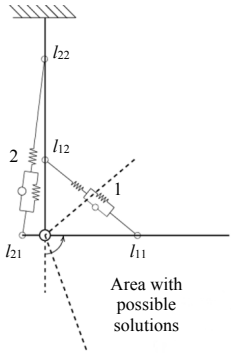

Fig. 3. Model of human elbow and range of motion with equilibrium solutions of the torques exerted by the muscles.

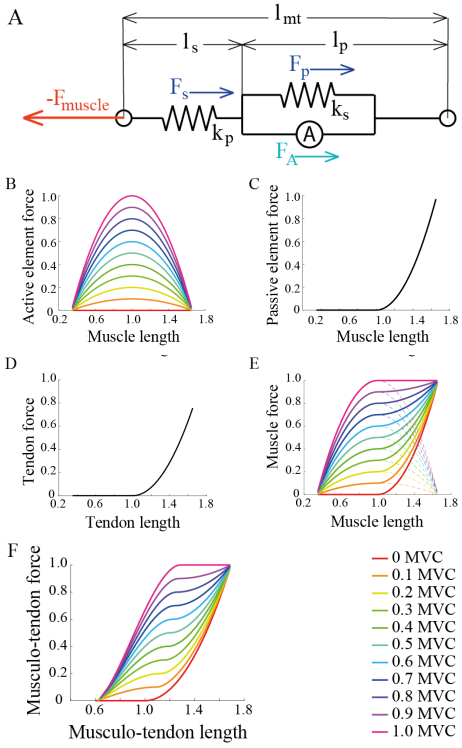

Fig. 4. Muscolo-tendon element characteristics.

The muscle (l_p) consists of an active element (A), representing the actin-myosin action, and a nonlinear spring in parallel with A (parallel spring) to model the collagen tissue. The tendon segment (l_s) is composed of a nonlinear spring (serial spring) in series with A. The laws that relate the forces exerted by the active element (F_A) and by the parallel spring (F_p) with the length of the muscle segment (l_p), and the force exerted by the serial spring (F_s) with the length of the tendon (l_s), together with their coefficients, are reported in Eqs. (1)–(3) (**Figs. 4B–D**) derived from the literature [42, 43].

$$F_A = m \cdot F_{MAX} \left[-a \left(\frac{l_p}{l_{ce}} \right)^2 + 2a \frac{l_p}{l_{ce}} - a + 1 \right] \quad . \quad (1)$$

$$F_s = k_s \left[\max \left(0, l_s - l_{s0} \right) \right]^2 \quad . \quad . \quad . \quad . \quad . \quad . \quad . \quad . \quad . \quad (2)$$

$$F_p = k_p \left[\max \left(0, \frac{l_p}{l_{ce}} - \frac{l_{p0}}{l_{ce}} \right) \right]^2 \quad . \quad . \quad . \quad . \quad . \quad . \quad . \quad (3)$$

where $a = 1/w^2$ and w is muscle width; m is muscle activation, measured as a fraction of the Maximum Voluntary Contraction (MVC); l_{ce} is the optimal length at which the muscle exerts its maximal active force (F_{MAX}); k_p is the stiffness of the muscle (chosen so that if $F_p = F_{MAX}$, the ratio $l_p/l_{ce} = 1 + w$); $l_{p0} = l_{ce}$ is the muscle relaxation length, indicating the maximum length of the muscle for which the parallel spring does not exerted any passive force; k_s is the tendon stiffness (chosen so that at F_{MAX}, $l_s = 1.04 l_{s0}$ [44]); and l_{s0} is the tendon slack length, indicating the maximum length of the tendon for which the serial spring does not exert any force. F_{MAX}, l_{ce}, and l_{s0} are muscle specific. Characteristic values and anthropometrical information related to the BRD and TriLat [45] are reported in **Table 1**.

Figures 4B–D are plots of the force exerted by the active element of the muscle, by the parallel spring, and by the serial spring in relation to their lengths at different activations. **Fig. 4E** illustrates the force exerted by the muscle element in relation to its length, and **Fig. 4F** illus-

Table 1. Anatomical parameters used in the study.

	1: BRD	2: TriLat
l_{ce} [m]	0.0858	0.1138
l_{p0} [m]	0.0858	0.1138
l_{s0} [m]	0.0535	0.0980
$F_{\max}$ [N]	261.33	624.3
k_p [N/m]	600	1433
k_s [N/m]	$163 \cdot 10^3$	$390 \cdot 10^3$
Attach on Radius-Ulna [m]	l_{11} : 0.1274	l_{21} : 0.0219
Attach on Humerus [m]	l_{12} : 0.1004	l_{22} : 0.1735

trates the force exerted by the musculo-tendon system in relation to its length.

5.2. Equations for Force Balancing

The joint axis of rotation was assumed to be vertical in order to neglect the gravity action. Eq. (4) describe the dynamic equilibrium:

$$\begin{cases} F_{s1} = F_{p1} + F_{A1} \\ F_{s2} = F_{p2} + F_{A2} \\ m_{a_2}(F_{p2} + F_{A2}) = m_{a_1}(F_{p1} + F_{A1}) \end{cases} \quad \ldots \quad (4)$$

where F_{si}, F_{pi}, F_{Ai}, and m_{a_i} are, respectively, forces exerted by the serial spring, by the parallel spring, by the active element, and by the moment arm of muscle force with respect to the elbow. The two muscles are indicated by $i = 1, 2$.

The force equations are coupled with geometrical equations, as follows:

$$\begin{cases} l_{mti} = l_{pi} + l_{si} \\ l_{mti} = \sqrt{l_{i1}^2 + l_{i2}^2 - 2 \cdot l_{i1} \cdot l_{i2} \cdot \cos\beta_i} \\ m_{a_i} = \dfrac{2}{l_{mti}} \sqrt{\dfrac{P_i}{2}\left(\dfrac{P_i}{2} - l_{i1}\right)\left(\dfrac{P_i}{2} - l_{i2}\right)\left(\dfrac{P_1}{2} - l_{mti}\right)} \end{cases} \quad (5)$$

5.3. Stiffness and Performance Calculations

Different levels of co-contraction are defined with respect to the activation of muscle 1. The rotational stiffness of the musculo-tendon system is defined as the derivative of displacement caused by imposed torque τ_i:

$$K_i = m_{a_i} \frac{\partial (F_{pi} + F_{Ai})}{\partial \alpha} + (F_{pi} + F_{Ai}) \frac{\partial m_{a_i}}{\partial \alpha} \quad \ldots \quad (6)$$

A small deflection ($\partial\alpha = 0.01°$) [10] is applied to the elbow joint in both positive and negative directions, while the muscle activations are not changed. Eq. (6) represents an estimation of the elbow stiffness in a particular pose.

The force exerted by the muscle depends on its length, and a corresponding torque is exerted at the elbow joint. The elbow angle-torque relation can be linearized around the unperturbed configuration, and the slope represents the stiffness of the muscles. The rotational stiffness of the elbow is the difference between the slopes of the elbow angle-torque curves of muscle 1 with respect to muscle 2. The performance is calculated as the ratio between the elbow stiffness, intended as the output of the system and the norm of the muscle activation, intended as the input of the model.

6. Analysis of the Model

6.1. Musculo-Tendon System Characteristics

Variations in the joint angle lead to different variations in the lengths of the antagonist muscles. Because the torque length of the muscle characteristic is specific for each muscle, this behavior could be interpreted as a shifting of the characteristic of one muscle along the other in order to match the lengths the two muscles assume at a specific joint angle (**Fig. 5**). We may observe that this shifting permits the two muscles to apply a force along the same range of angles (between 20° and 130°), even if they exert force along different ranges of length (between 0.09 and 0.20 m for muscle 1 and between 0.17 and 0.21 m for muscle 2).

6.2. Elbow Angle Boundaries

The range of the angles the elbow may assume, owing to physiological boundaries, is reported in [46]. However, other boundaries owing to the muscle force exertion characteristic may be identified. Thus, the physiological boundaries and the boundaries resulting from the muscle characteristic may not coincide. In **Fig. 6A**, the upper value of the elbow flexion is fixed at 130° owing to a physiological boundary.

However, possible solutions for co-contraction can also be obtained for higher elbow flexion values. However, extant studies identified the lower boundary close to 0° although no possible intersection between the characteristics of the two muscles of our model are possible below 20°. This discrepancy may result from the approximation of the muscle model or because those other muscles acting on the same elbow joint that are neglected in this model.

It can be observed that the activations of the antagonist muscles univocally identify the elbow flexion if no torque is exerted by the elbow joint.

6.3. Antagonist Muscle Activation

In **Fig. 6B**, the activation of muscle 2, which ensures the equilibrium at the elbow, is represented at different elbow configurations and muscle 1 activations. Curves regarding the low activation of muscle 1 are more sparse with respect to curves for the higher activation of muscle 1. For this reason, the steps between muscle 1 activations in this and the following figures are not constant. An indifferent equilibrium is possible for angles lower than 85°, where both muscles are maintained with no activation.

Activating muscle 2 is always necessary for elbow flexions higher than 85° to compensate the force exerted by the passive element of muscle 1.

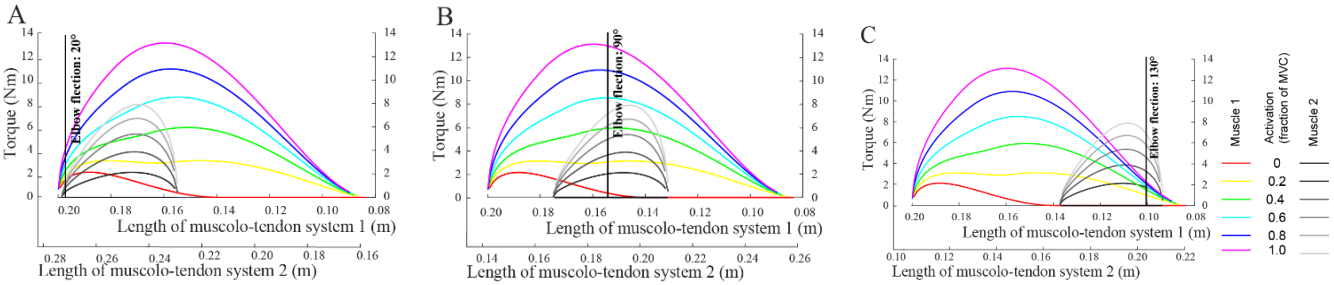

Fig. 5. Intersections between the characteristics of the torque, related to the musculo-tendon length, exerted by the two muscles for different elbow flexion, at different level of activation of muscle 1 (colored) and 2 (gray scale).

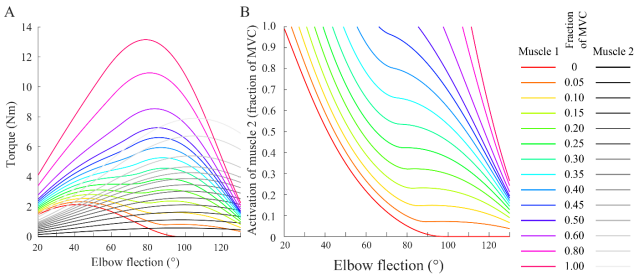

Fig. 6. Elbow torque and activation of muscle 2 to balance muscle 1 torque: A. torque vs elbow flexion; B. Muscle 2 activation vs elbow flexion.

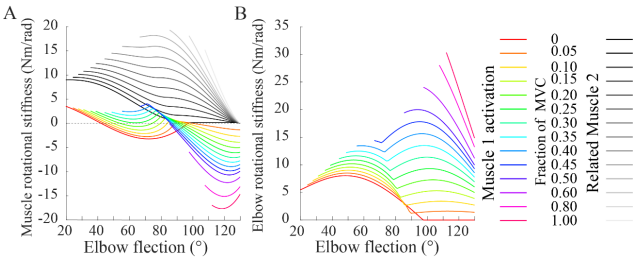

Fig. 7. Muscles and elbow stiffness vs elbow flexion. A. Rotational stiffness of the muscles. B. Rotational stiffness of the elbow and muscle 1 activations.

Not all possible elbow flexions and muscle 1 activations are feasible together. In particular, higher activations of muscle 1 are balanced by muscle 2 only for higher values of elbow flexion. Lower activations of muscle 2 are balanced by muscle 1 only for lower values of elbow flexion. These boundaries define a range of muscle activations in which the stiffening of the elbow, without exerting torque, is possible.

6.4. Arm Stiffness

The stiffness of the two muscles is reported in **Fig. 7A**. While the stiffness of muscle 2 is always nonnegative, the stiffness of muscle 1 can assume negative values. This behavior can be physiological and is a consequence of the negative slope of the elbow flexion-torque relation (see **Fig. 6A**), which leads to the exertion of lower torques for higher lengths of the musculo-tendon system.

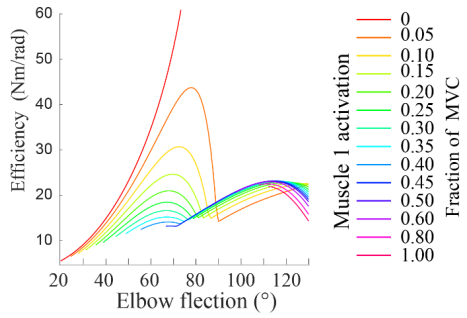

Fig. 8. Relation of performance and elbow flexion for different values of muscle 1 activations.

The joint stiffness increases with the muscle activation for each elbow angle (**Fig. 7B**). Two peaks can be found owing to the passive and active elements of muscle 1. Because the balancing of torque exerted by the high activation of muscle 1 is possible only at some joint angles, the stiffness of higher muscle activations can be computed only for these angles. There exist some elbow flexions at which both muscles are not activated. In these cases, a range of angles at which the stiffness is null can be found.

6.5. Performance

The performance, intended as the ratio between the elbow stiffness and the norm of muscle activations (**Fig. 8**), indicates minima between 70° and 90°. These minima depend on the muscle activations and are found in correspondence of the joint angle at which the parallel spring of muscle 1 starts its action. Two peaks are found, except for the muscle activation equal to zero. The first peak corresponds to joint angles at which the parallel spring of muscle 1 exerts a passive force (lower joint angles). The second peak corresponds to joint angles at which the parallel spring of muscle 1 does not exert any force (higher joint angles). Thus, we can find a range in which the system is more effective in stiffening the joint.

7. Discussion and Conclusions

This study is a preparatory phase for the development of an exoskeleton for industrial use, whose stiffness can

be controlled in real time with the operator's arm stiffness, calculated from the muscle activation recorded with electromyography. In this study, a model for the evaluation and analysis of elbow stiffness was presented. This model can be successively implemented and used for the study of the control law of the exoskeleton.

The muscle model used in this study is a simple approximation of a real muscle. However, since the purpose of this model is to approximate the mechanical characteristics of arm stiffness, and not to study the specific properties of the muscle itself, we may assume that the approximations of the present model are acceptable in relation to its purpose [47].

We also introduced an estimation of the performance related to the elbow angle, and an analysis of the performance of the human elbow that would be coupled with the exoskeleton. This estimation could be useful in defining the configuration the subject has to assume in order to reduce his/her muscle activation without reducing the exerted endpoint stiffness.

In future work, we plan to complete the model by adding another joint, modeling the shoulder, and increasing the redundancy of the system by adding more muscles and using physiological laws to select the muscle activations. Increasing the number of joints will result in the occurrence of singularities. However, poses in which singularities would occur are deprecated, and the operator is recommended not to operate in those poses. This model would be used to test the control law implemented in the exoskeleton.

References:

[1] E. E. Cavallaro, J. Rosen, J. C. Perry, and S. Burns, "Real-time myoprocessors for a neural controlled powered exoskeleton arm," IEEE Trans. Biomed. Eng., Vol.53, pp. 2387-2396, November 2006.

[2] J. Rosen, M. Brand, M. B. Fuchs, and M. Arcan, "A myosignal-based powered exoskeleton system," IEEE Trans. Syst. Man, Cybern. - Part A Syst. Humans, Vol.31, pp. 210-222, May 2001.

[3] E. Rocon, J. M. Belda-Lois, A. F. Ruiz, M. Manto, J. C. Moreno, and J. L. Pons, "Design and validation of a rehabilitation robotic exoskeleton for tremor assessment and suppression," IEEE Trans. Neural Syst. Rehabil. Eng., Vol.15, pp. 367-378, September 2007.

[4] B. J. Makinson, "Research and Development Prototype for Machine Augmentation of Human Strength and Endurance. Hardiman I Project," General Electric Report S-71-1056, Schenectady, NY, May 1971.

[5] A. Young and D. Ferris, "State-of-the-art and Future Directions for Robotic Lower Limb Exoskeletons," IEEE Trans. Neural Syst. Rehabil. Eng., Vol.25, No.2, pp. 171-182, February 2017.

[6] A. B. Zoss, H. Kazerooni, and A. Chu, "Biomechanical design of the Berkeley lower extremity exoskeleton (BLEEX)," IEEE/ASME Trans. Mechatr., Vol.11, pp. 128-138, April 2006.

[7] S. K. Banala, S. H. Kim, S. K. Agrawal, and J. P. Scholz, "Robot assisted gait training with active leg exoskeleton (ALEX)," IEEE Trans. Neural Syst. Rehab. Eng., Vol.17, pp. 2-8, Feb. 2009.

[8] T. Nef, M. Mihelj, and R. Riener, "ARMin: a robot for patient-cooperative arm therapy," Med. Biol. Eng. Comput., Vol.45, pp. 887-900, September 2007.

[9] S. Zhou, D. L. Lawson, W. E. Morrison, and I. Fairweather, "Electromechanical delay in isometric muscle contractions evoked by voluntary, reflex and electrical stimulation," Eur. J. Appl. Physiol. Occup. Physiol., Vol.70, No.2, pp. 138-145, March 1995.

[10] K. Sacco, F. Cauda, F. D'Agata, S. Duca, M. Zettin, R. Virgilio et al., "A combined robotic and cognitive training for locomotor rehabilitation: evidences of cerebral functional reorganization in two chronic traumatic brain injured patients," Front. Hum. Neurosci., Vol.5, p. 146, November 2011.

[11] J. van der Vorm, R. Nugent, and L. O'Sullivan, "Safety and Risk Management in Designing for the Lifecycle of an Exoskeleton: A Novel Process Developed in the Robo-Mate Project," Procedia Manuf., Vol.3, pp. 1410-1417, July 2015.

[12] S. Spada, L. Ghibaudo, S. Gilotta, L. Gastaldi, and M. P. Cavatorta, "Measurement procedure of parameter to assess an exoskeleton introduction in industrial reality: main issues and EAWS risk assessment," Proc. Manuf., 2017.

[13] N. Sylla, V. Bonnet, F. Colledani, and P. Fraisse, "Ergonomic contribution of ABLE exoskeleton in automotive industry," Int. J. Ind. Ergon., Vol.44, pp. 475-481, July 2014.

[14] T. Flash, "The control of hand equilibrium trajectories in multi-joint arm movements," Biol. Cybern., Vol.57, pp. 257-274, November 1987.

[15] E. Burdet, R. Osu, D. Franklin, T. Milner, and M. Kawato, "The central nervous system stabilizes unstable dynamics by learning optimal impedance," Nature, Vol.414, pp. 446-449, November 2001.

[16] R. Shadmehr, F. A. Mussa-Ivaldi, and E. Bizzi, "Postural force fields of the human arm and their role in generating multijoint movements," J. Neurosci., Vol.13, pp. 45-62, January 1993.

[17] E. J. Perreault, R. F. Kirsch, and P. E. Crago, "Voluntary Control of Static Endpoint Stiffness During Force Regulation Tasks," J Neurophysiol, Vol.87, pp. 2808-2816, June 2002.

[18] D. Franklin and T. Milner, "Adaptive control of stiffness to stabilize hand position with large loads," Exp. Brain Res., Vol.152, No.2, pp. 211-220, July 2003.

[19] N. Hogan, "Impedance control: An approach to manipulation," Am. Control Conf. 1984, June 1984.

[20] T. Yoshikawa, "Manipulability of Robotic Mechanisms," Int. J. Rob. Res., Vol.4, pp. 3-9, June 1985.

[21] M. Verotti, P. Masarati, M. Morandini, and N. P. Belfiore, "Isotropic compliance in the Special Euclidean Group SE(3)," Mech. Mach. Theory, Vol.98, pp. 263-281, April 2016.

[22] M. Verotti and N. P. Belfiore, "Isotropic Compliance in $E(3)$: Feasibility and Workspace Mapping," J. Mech. Robot., Vol.8, No.6, September 2016.

[23] F. Mussa-Ivaldi, N. Hogan, and E. Bizzi, "Neural, mechanical, and geometric factors subserving arm posture in humans," J. Neurosci., Vol.5, pp. 2732-2743, October 1985.

[24] P. L. Gribble, L. I. Mullin, N. Cothros, and A. Mattar, "Role of cocontraction in arm movement accuracy," J. Neurophysiol, Vol.89, No.5, pp. 2396-2405, May 2003.

[25] R. Osu, N. Kamimura, H. Iwasaki, E. Nakano, C. M. Harris, Y. Wada, and M. Kawato, "Optimal impedance control for task achievement in the presence of signal-dependent noise," J. Neurophysiol, Vol.92, No.2, pp. 1199-1215, August 2004.

[26] H. Gomi and R. Osu, "Task-dependent viscoelasticity of human multijoint arm and its spatial characteristics for interaction with environments," J. Neurosci., Vol.18, pp. 8965-8978, November 1998.

[27] R. Osu and H. Gomi, "Multijoint muscle regulation mechanisms examined by measured human arm stiffness and EMG signals," J. Neurophysiol., Vol.81, pp. 1458-1468, April 1999.

[28] M. Mauro, S. Mohtar, T. Pastorelli, and S. Sorli, "Pre-design of an active central mechanism for space docking," 67th Int. Astronautical Congr. (IAC 2016), October 2016.

[29] J. F. Veneman, R. Kruidhof, E. E. G. Hekman, R. Ekkelenkamp, E. H. F. Van Asseldonk, and H. van der Kooij, "Design and Evaluation of the LOPES Exoskeleton Robot for Interactive Gait Rehabilitation," IEEE Trans. Neural Syst. Rehabil. Eng., Vol.15, pp. 379-386, September 2007.

[30] T. Lenzi, N. Vitiello, S. M. M. De Rossi, S. Roccella, F. Vecchi, and M. C. Carrozza, "NEUROExos: A variable impedance powered elbow exoskeleton," 2011 IEEE Int. Conf. on Robotics and Automation, pp. 1419-1426, May 2011.

[31] A. Ajoudani, N. Tsagarakis, and A. Bicchi, "Tele-impedance: Teleoperation with impedance regulation using a body-machine interface," Int. J. Rob. Res., Vol.31, pp. 1-14, October 2012.

[32] P. Liang, C. Yang, N. Wang, Z. Li, R. Li, and E. Burdet, "Implementation and test of human-operated and human-like adaptive impedance controls on Baxter robot," Conf. on Advances in Autonomous Robotics Systems (TAROS 2014), pp. 109-119, September 2014.

[33] M. Ison and P. Artemiadis, "Multi-directional impedance control with electromyography for compliant human-robot interaction," IEEE Int. Conf. Rehab. Robotics, pp. 416-421, October 2015.

[34] A. A. Blank, A. M. Okamura, and L. L. Whitcomb, "Task-dependent impedance and implications for upper-limb prosthesis control," Int. J. Rob.control, Vol.33, pp. 827-846, May 2014.

[35] S. Lee and Y. Sankai, "Virtual impedance adjustment in unconstrained motion for an exoskeletal robot assisting the lower limb," Adv. Robot., Vol.19, pp. 773-795, January 2005.

[36] F. Lacquaniti, M. Carrozzo, and N. A. Borghese, "Time-varying mechanical behavior of multijointed arm in man," J. Neurophysiol., Vol.69, pp. 1443-1464, May 1993.
[37] H. Gomi and M. Kawato, "Equilibrium-point control hypothesis examined by measured arm stiffness during multijoint movement," Science, Vol.272, pp. 117-120, April 1996.
[38] L. P. J. Selen, D. W. Franklin, and D. M. Wolpert, "Impedance control reduces instability that arises from motor noise," J. Neurosci., Vol.29, pp. 12606-12616, October 2009.
[39] D.-Z. Chen and K.-L. Yao, "Drive train design of redundant-drive backlash-free robotic mechanisms," Mech. Mach. Theory, Vol.35, pp. 1269-1285, September 2000.
[40] D.-Z. Chen, C.-P. Liu, and D.-W. Duh, "On the conceptual design of redundant-drive backlash-free geared robot manipulators," Mech. Mach. Theory, Vol.37, pp. 3-14, January 2002.
[41] A. V. Hill, "The Mechanics of Active Muscle," Proc. R. Soc. B Biol. Sci., Vol.141, pp. 104-117, March 1953.
[42] D. Borzelli, S. Pastorelli, and L. Gastaldi, "Model of the human arm stiffness exerted by two antagonist muscles," 25th Int. Conf. on Robotics in Alpe-Adria-Danube Region, November 2016.
[43] D. Borzelli, S. Pastorelli, and L. Gastaldi, "Determination of the Human Arm Stiffness Efficiency with a Two Antagonist Muscles Model," in Mechanisms and Machine Science, pp. 71-78, November 2017.
[44] D. A. Kistemaker, J. D. Wong, and P. L. Gribble, "The central nervous system does not minimize energy cost in arm movements," J. Neurophysiol., Vol.104, pp. 2985-2994, December 2010.
[45] K. R. S. Holzbaur, W. M. Murray, and S. L. Delp, "A Model of the Upper Extremity for Simulating Musculoskeletal Surgery and Analyzing Neuromuscular Control," Ann. Biomed. Eng., Vol.33, pp. 829-840, June 2005.
[46] J. P. Iannotti and R. D. Parker, "The Netter Collections of Medical Illustrations: Musculoskeletal System, part I – Upper Limb," 2nd ed., Vol.6. Philadelphia, PA: Saunders, 2013.
[47] J. M. Inouye and F. J. Valero-Cuevas, "Muscle Synergies Heavily Influence the Neural Control of Arm Endpoint Stiffness and Energy Consumption," PLoS Comput. Biol., Vol.12, p. e1004737, February 2016.

Name:
Daniele Borzelli

Affiliation:
Department of Mechanical and Aerospace Engineering, Politecnico di Torino

Address:
Corso Duca degli Abruzzi 24, 10129, Turin, Italy

Brief Biographical History:
2014- Ph.D Student, Mechanical Engineering, Politecnico di Torino
2010- Research at the Neuro-Physiology Laboratory, IRCCS Fondazione Santa Lucia
2010 Received Master degree in Mechanical Engineering, 'La Sapienza,'

Name:
Stefano Pastorelli

Affiliation:
Department of Mechanical and Aerospace Engineering, Politecnico di Torino

Address:
Corso Duca degli Abruzzi 24, 10129 Torino, Italy

Brief Biographical History:
1996 Received Ph.D. in Applied Mechanics
2005- Associate Professor, Applied Mechanics and Robotics, Politecnico di Torino

Main Works:
• L. Gastaldi, G. Lisco, and S. Pastorelli, " Evaluation of functional methods for human movement modeling," Acta Bioeng Biomech, Vol.17, pp. 31-38, 2015.
• M. Galetto, L. Gastaldi, G. Lisco, L. Mastrogiacomo, and S. Pastorelli, "Accuracy evaluation of a new stereophotogrammetry-based functional method for joint kinematic analysis in biomechanics," Proc IMechE Part H, J. Engineering in Medicine, Vol.228, No.11, pp. 1183-1192, 2014.
• C. Ferraresi, M. Paoloni, S. Pastorelli, and F. Pescarmona, "A new 6-DOF parallel robotic structure actuated by wires: the WiRo-6.3," J. Robotic Syst., Vol.21, No.11, pp. 581-595, 2004.
• Functional design of mechanical systems, kinematics and dynamics of robots, 3-D motion capture techniques and identification, active human modelling for biomechanics, human-machine interfaces and collaborative robotics

Membership in Academic Societies:
• American Society of Mechanical Engineering (ASME)
• International Society of Biomechanics (ISB)

Name:
Laura Gastaldi

Affiliation:
Department of Mechanical and Aerospace Engineering, Politecnico di Torino

Address:
Corso Duca degli Abruzzi 24, 10129 Torino, Italy

Brief Biographical History:
1993 Received Master degree in Mechanical Engineering
1998 Received Ph.D. in Applied Mechanics
2000- Assistant Professor of Applied Mechanics, Politecnico di Torino

Membership in Academic Societies:
• International Society of Biomechanics (ISB)